Effect of the initial particles size distribution on the properties of suspension plasma sprayed Al_2O_3-TiO_2 coatings

M. Vicent[1,*], E. Bannier[1], P. Carpio[1], E. Rayón[2], R. Benavente[2], M. D. Salvador[2], E. Sánchez[1]

[1] Instituto de Tecnología Cerámica (ITC), Asociación de Investigación las Industrias Cerámicas (AICE), Universitat Jaume I (UJI), Av. Vicent Sos Baynat s/n, 12006 Castellón, Spain

[2] Instituto de Tecnología de Materiales (ITM), Universitat Politècnica de València (UPV), Camino de Vera s/n, 46022 Valencia, Spain

[(*)]Mónica Vicent: corresponding author

Mailing address: Instituto de Tecnología Cerámica. Campus Universitario Riu Sec. Av. Sos Baynat s/n, 12006 Castellón (Spain).

Telephone: +34 964342424

Fax: +34 964342425

E-mail: monica.vicent@itc.uji.es

Emilie Bannier (e-mail: emilie.bannier@itc.uji.es)

María Dolores Salvador (e-mail: dsalva@mcm.itm.es)

Amparo Borrell (e-mail: aborrell@itm.es)

Enrique Sánchez (e-mail: enrique.sanchez@itc.uji.es)

Abstract

Al_2O_3-TiO_2 coatings have been deposited by atmospheric plasma spraying from agglomerated nanostructured powders showing better properties than their conventional (microstructured) counterparts. These coatings can be also obtained by suspension plasma spraying however the research on suspension plasma sprayed Al_2O_3-TiO_2 is still scarce. Consequently, it is crucial to study the effect of the suspension characteristic on the coating properties and to optimise the deposition process.

In this work, Al_2O_3-13wt%TiO_2 tribological coatings were successfully deposited by suspension plasma spraying from three different feedstocks: a nanometric suspension and two bimodal suspensions with different solid contents made up of titania nanoparticles and alumina submicron-sized particles. The coatings microstructure and phase composition were characterised using electronic microscopy and X-ray diffraction analysis. Moreover, nanoindentation technique was used to determine the coatings mechanical properties.

The influence of the feed suspension characteristics on the final coating quality was analysed. Findings showed that similar microstructures and phases were evolved after depositing the different feedstocks. In addition suspension feedstock made up of nanoparticles resulted in a coating with better mechanical properties. However the use of submicron-sized particles in the suspension feedstocks gives rise to some technical and economic advantages in the process which should be taking into account when a SPS process is to be set up.

Keywords: Suspension Plasma Spraying; Alumina-Titania; Microstructure; Indentation

1 Introduction

A possible way to obtain nanostructured coatings by thermal spraying [1-5] consists of using a carrier liquid instead of a carrier gas to inject the nanoparticles inside the plasma plume [2]. This technique is known as Suspension Plasma Spraying (SPS) and differs significantly from conventional APS since the suspension is fragmented into droplets and the liquid phase vaporised before the solid feedstock is processed [6,7]. This novel technique has recently undergone an extensive development, leading to the deposition of nanostructured coatings with unique properties and new functionalities [8-11].

Among the materials usually deposited by plasma spraying, alumina-based coatings show one of the most versatile fields of application [12]. Alumina is commonly used as an electrical insulator due to its high dielectric strength and its ability to manufacture hard and chemically stable coatings even at very high temperatures. However, its lack of toughness and flaw tolerance constrains some properties such as thermal shock resistance. Still, Al_2O_3-based coatings are widely used for wear, corrosion or erosion protection components. In such coating, alumina is mixed with other oxides to enhance its properties. It has been shown that the addition of TiO_2 improves the coating fracture toughness in conventional APS coatings [12]. Indeed Al_2O_3-TiO_2 coatings obtained by APS from both conventional or nanostructured, agglomerated feedstock powders has been extensively studied [13-17]. In this previous research Al_2O_3-TiO_2 coatings deposited from nanopowders have shown very promising bonding strength and wear resistance compared with conventional feedstock [18]. Moreover, the Al_2O_3-TiO_2 mixture with 13 wt% of TiO_2 displayed the best wear resistance among all the nanostructured Al_2O_3-TiO_2 coatings [19]. However, the research on Al_2O_3-TiO_2 coatings by SPS is still incipient and very few authors have studied such layers [20]. Consequently, it is still necessary to study the effect of the characteristics of the

feedstock on the final coating microstructure and properties in SPS Al_2O_3-TiO_2 coatings.

In SPS process ethanol has been more extensively used as suspension solvent due to its lower vaporisation heat but water is preferable for sustainability reasons [21]. Although in principle higher solids content can be desirable in terms of deposition efficiency this content must be optimised to avoid clogging during injection as well as incomplete particle melting inside plasma torch. With regard to particle size in the suspension feedstock, SPS technology ranges from few tens of nanometers to few microns. When nanoparticles are used a much higher tendency to agglomerate is observed. Besides the particle melting in plasma torch is also deeply affected by the particle size distribution. Thus excessively small particles do not flatten so effectively meanwhile large particles and agglomerates display higher tendency to remain partly unmelted [2]. Few attempts have been made to use feedstock mixtures of different particle size distributions, e.g. submicron-nano sized particles despite their many potential advantages. The use of such bimodal distribution comprising the feedstock suspension can give rise to significant benefits during the suspension processing, i.e. higher solids content and lower viscosity leading to better feeding in the plasma torch along with higher deposition efficiency [22]. Besides some coatings properties can be improved when using bimodal feedstock as recently reported for APS coatings [8,9]. However, the use of these bimodal powders has hardly been treated in SPS literature.

Standard SPS process results in thinner coatings than those obtained by conventional APS process. As a consequence it has been successfully proved that nanoindentation technique is a more feasible method than conventional microindentation for the mechanical characterisation of such layers. However, the amount of papers dealing with the use of nanoindentation method to characterise SPS layers is still very scarce [23].

In this work, Al_2O_3-13wt%TiO_2 tribological coatings were successfully deposited by SPS from three different feedstocks: a nanometric suspension and two bimodal suspensions with different solid contents made up of titania nanoparticles and alumina submicron-sized particles. The coatings microstructure and phase composition were characterised using electronic microscopy and X-ray diffraction analysis. Moreover, nanoindentation technique was used to determine the coatings mechanical properties.

2 Materials and methods

2.1 Feedstocks preparation

Two commercial nanopowder suspensions of alumina and titania (VP Disp. W630X and AERODISP® W740X respectively, Degussa-Evonik, Germany), a submicron-sized powder of alumina (Condea-Ceralox HPA-0.5, Sasol, USA) and a nanopowder of titania (AEROXIDE® P25, Degussa-Evonik, Germany) were used as raw materials. Both suspensions have been fully characterised in previous works [24-26]. Table 1 shows the main characteristics of the suspensions and powders used to prepare the different feedstocks.

First, a 10 vol.% of 87 wt% Al_2O_3–13 wt% TiO_2 nanosuspension was prepared by mixing both commercial suspensions [4,24]. This suspension was referenced as N10. Secondly, one 10 vol.% and one 15 vol.% of 87 wt% Al_2O_3–13 wt% TiO_2 submicron-nano suspension were prepared by dispersing nanosized titania particles and submicronic alumina particles in water [26]. These suspensions were designed as SN10 and SN15 respectively. A commercial polyacrylic acid-based polyelectrolyte (DURAMAX™ D-3005, Rohm & Haas, USA) was used as deflocculant [26]. In both cases, stable, well-dispersed and low-viscosity suspensions were obtained, following the methodology described elsewhere [4,24,26]. Figure 1 details a flow diagram describing

the suspension preparation routes followed to obtain the three suspension feedstocks. Rheological behaviour of all the prepared suspensions was previously determined using a rheometer, demonstrating that the incorporation of submicron sized particles leads to a significant reduction of viscosity, as expected for the lower surface area of those particles [27]. Also in previous research of the authors the stability of these three feedstocks was proven [4,24,26].

Stainless steel (AISI 304) disks have been used as substrates (25 mm diameter and 10 mm thickness). Before deposition, the substrates were grit blasted with corundum (Metcolite VF, Sulzer Metco, Switzerland) at a pressure of 4.2 bar and cleaned with ethanol.

2.2 Coating deposition

Coatings were deposited with a monocathode torch (F4-MB, Sulzer Metco, Switzerland) with a 6 mm internal diameter anode operated by a robot (IRB 1400, ABB, Switzerland). The substrates were preheated between 350 ºC and 400 ºC to enhance coating adhesion.

The suspensions were injected using a SPS system developed by the Institute for Ceramic Technology (Instituto de Tecnología Cerámica, ITC). This system is formed by two pressurised containers which force the liquid to flow through the injector. A filter was used to remove agglomerates larger than 75 μm and possible contaminations. Main spraying parameters are given in table 2.

2.3 Coating characterisation techniques

X-ray diffraction patterns were collected to identify crystalline phases in coating samples (Theta-Theta D8 Advance, Bruker, Germany). The microstructure was analysed on polished cross-sections using an Electronic Microscope, SEM (JSM6300,

Jeol. Japan). Finally, elemental analysis was performed in SEM using energy dispersive X-rays analysis (EDX).

Coating's hardness and elastic modulus were acquired by a nanoindenter (G-200, Agilent Technology, USA). Indentations were performed at 2000 nm constant depth using the Continuous Stiffness Measurement (CSM) method. A Berkovich diamond tip was used after the area function calibration procedure on fused silica was carried out assuring a tip radius below 100 nm. Average values of hardness and elastic modulus were then determined for a depth range from 100 to 200 nm. More details of this procedure can be found in previous research [21,23].

3 Results and discussion

3.1 Coatings microstructure

Figure 2 shows the cross-sectional SEM micrographs of the as-sprayed coatings obtained from the three different feedstocks. All the coatings display a microstructure formed by melted and partially melted areas as reported elsewhere [21,23]. This microstructure develops because after the liquid is evaporated the resulting particles or agglomerates may thus be heated, partly melted, or melted, yielding the end coating. Overall no significant differences were found coating microstructure by introducing submicron particles in the starting suspension, but as expected this submicron-sized particles addition leads to the presence of larger particles in partially melted areas of the coating (SN10 and SN15). In addition, it should be noted that the increase of suspension concentration (from SN10 to SN15) does not change the microstructure of the resulting coating but allows thicker coatings to be obtained (from 30 to 55 μm) giving rise to an improvement of process efficiency.

To assess the homogeneity of alumina-titania distribution in the coating EDX analysis was carried out for the three coatings. For the sake of simplicity figure 4 describes only the analysis corresponding to N10 coating since similar analysis were obtained for the other two samples. As it can be observed alumina and titania phases are homogeneously deposited throughout the coating. These findings indicate that the preparation of the suspension feedstocks is crucial to obtain a homogeneous distribution of the compounds in the final coating [4,27,28]. If this preparation is adequate the characteristics of the suspension feedstock, i.e solids concentration or particle size distribution does not seem to affect on coating homogeneity in terms of phases distribution.

Finally, XRD patterns of all coatings are shown in figure 5. As it can be observed the alumina found in the three coating is mainly present as corundum and gamma alumina, independently of feed material phases since nanometric alumina is formed by transition phases (δ- and γ-Al_2O_3) and submicron-sized alumina is exclusively corundum (α-Al_2O_3). For this reason, the amount of preserved corundum grows in the coatings containing submicron-sized particles (samples SN10 and SN15). In respect of titania, most of the initial phase (an anatase:rutile ratio of approximately 3:1) reacts with alumina during the deposition process, leading to the formation of aluminium titanate (tialite). This finding confirms the intimate mixture of compounds in the starting suspensions in a SPS process since similar compositions of alumina-titania sprayed in powder form (APS process) react in less extent to form these titanates compounds [28].

3.2 Coatings nanomechanical properties

Nanomechanical properties were measured by nanoindentation with a Berkovich indenter. The hardness and elastic modulus values and their corresponding error bars for the three coating are shown in figure 6. The averaged hardness and elastic modulus values were detailed in table 3.

These results reveal that mechanical properties are significantly better (around 30% higher) for the coating prepared from nanoparticles (N10). Thus this finding confirms previous research when nanostructured feedstocks have been used in APS processes [27-29]. As this literature states submicron-structured matrices comprising coatings obtained from nanostructured feedstocks results in coatings with better mechanical properties provided that the amount and poor cohesion of unmolten zones do not compensate the enhancement matrix effect. However, although the number of papers about mechanical properties in alumina-titania coatings, obtained from nanostructured feedstocks by APS process, is abundant; no papers on SPS coatings from nano- or submicron-sized alumina-titania feedstocks addressing mechanical properties have been found. In one previous paper similar comparison of nanoindentation mechanical properties in alumina-titania coatings obtained from nano- and submicron-sized suspensions was carried out but the authors obtained the coatings by HVSFS (High Velocity Suspension Plasma Flame Spraying) [30]. Nevertheless this paper highlights an important issue in SPS coatings since the authors did not found differences in the mechanical properties of the coatings obtained either from nano- or submicron-sized feedstocks owing to the agglomeration state of nanoparticles in the suspension feedstock. In the present research the dispersion and stabilisation of the suspension feedstocks was previously set out [24,26]. For this reason the effect of nanoparticles on mechanical properties in N10 coating could be fully developed. In addition, previous research on nanoindentation in SPS coatings obtained from nanoparticle suspension feedstocks of other oxides such as YSZ or titania highlighted the enhanced mechanical properties found when nanoparticles suspensions were used as a consequence of the ultrafine character of SPS coating splats [21,23]. These papers also showed the mechanical weakening effect of the partially molten areas which appear in more or less

extent in SPS coatings. Further research is still necessary to confirm these preliminary findings, and more importantly, to establish a clear relation between coating microstructure and mechanical properties.

Finally, regarding SN coatings, an increase of suspension concentration did not modify mechanical properties of the coatings what could be considered, in principle, a positive effect if an optimisation of the solids concentration in the feedstock suspension is targeted as a consequence of the possible technical and economic benefits set out above.

3.3 Assessment of solids concentration effect in terms of energy consumption in aqueous suspensions

As set out above different solids concentration were used in two of the suspension feedstocks (SN10 and SN15). Thus increasing solids concentration gave rise to higher coating thickness when the same spraying conditions were used. Additionally, another benefit could be expected when higher solids concentration is used in the suspension feedstocks. This benefit relates to energy consumption associated to water vaporisation during plasma heating. In this sense changes in suspension powder concentration affect the total enthalpy needed to melt the solid: the solid fusion enthalpy increases when solid content also increases. However, the total enthalpy of the SPS process comprises two terms: fused solid enthalpy and liquid vaporisation heat. As reported in literature when ethanol is used as suspension solvent it is necessary to increase the deposition efficiency by using higher power to compensate the energy lost associated with the liquid vaporisation [2,31]. However when water is used the vaporisation heat is much higher than that of ethanol what can result in a different effect.

In order to explain this hypothesis, a simple equation derivated from energy balances of both phenomena produced during SPS (solid fusion and liquid evaporation) can easily be deduced (equation 1):.

$$\Delta H_{total} = w_{liquid} \cdot \Delta H_{V,liquid} + w_{solid} \cdot \Delta H_{F,solid} \quad \text{(Eq. 1)}$$

where ΔH is enthalpy and *w* is mass fraction of suspension component

Figure 3 plots the total enthalpy, ΔH_{total} which means the total energy required to vaporise two different solvents, water or ethanol as well as to melt the solid mixture (alumina:titania in weight ratio 87:13) versus solid content represented as the solid mass fraction (w_{solid}) present in the suspension feedstock [32,33]. Although the solid fusion enthalpy increases when solid content increases:

- Using ethanol as solvent, the enthalpy for vaporising ethanol is lower than the enthalpy for melting alumina-titania mixture.
- Using water as solvent, the enthalpy for vaporising water is higher than the enthalpy for melting alumina-titania mixture.

For this reason, unlike ethanol suspensions when water is used the total enthalpy decreases as the solids content in the suspension grows. An energy saving can be deduced for this estimate. However, other processing aspects should be taken into account when solids concentration is augmented such as the suspension stabilisation or the nozzle clogging during the suspension feeding in the torch.

4 Conclusions

Al_2O_3-TiO_2 coatings were successfully deposited by SPS from suspensions in which particle size (nano- and submicron-sized particles) and solids concentration were varied. Findings showed that similar microstructures comprising molten matrices and partially molten zones as well as phase distributions in the coatings were obtained. In addition the titania phase developed was homogenously distributed throughout the coating. On the other hand suspension feedstock made up of nanoparticles resulted in a coating with better mechanical properties than those obtained from submicron-sized particles. No

effect of solids concentration in submicron-sized feedstocks on coating mechanical properties was observed. However the use of submicron-sized particles to obtain suspension feedstocks with high solids concentration proved to give rise to some technical (improved processability) and economic (lower energy consumption) advantages in the SPS process which should be taken into account when a SPS process is to be set up.

Acknowledgements

This work has been supported by the Spanish Ministry of Science and Innovation (project MAT2012-38364-C03).

References

[1] A.K. Keshri, A. Agarwal, Plasma processing of nanomaterials for functional applications–A review, Nanosci. Nanotechnol. Lett. 4 (2012) 228–250.

[2] P. Fauchais, G. Montavon, R.S. Lima, B.R. Marple, Engineering a new class of thermal spray nano–based microstructures from agglomerated nanostructured particles, suspensions and solutions: An invited review, J. Phys. D: App. Phys. 44 (9) (2011) 93001.

[3] B.R. Marple, R.S. Lima, Engineering nanostructured thermal spray coatings: Process–property–performance relationships of ceramic based materials, Adv. App. Ceram. 106 (5) (2007) 265–275.

[4] E. Sánchez, A. Moreno, M. Vicent, M.D. Salvador, V. Bonache, E. Klyatskina, I. Santacruz, R. Moreno, Preparation and spray drying of Al_2O_3–TiO_2 nanoparticle suspensions to obtain nanostructured coatings by APS, Surf. Coat. Technol. 205 (4) (2010) 987–992.

[5] E.H. Jordan, M. Gell, Y.H. Sohn, D. Goberman, L. Shaw, S. Jiang, M. Wang, T.D. Xiao, Y. Wang, and P. Strutt, Development and implementation of plasma sprayed nanostructured ceramic coatings, Surf. Coat. Technol. 146–147 (2001) 48–54.

[6] L. Pawlowski, Suspension and solution thermal spray coatings, Surf. Coat. Technol. 203 (19) (2009) 2807–2829.

[7] R. Vassen, H. Kassner, G. Mauer, D. Stöver, Suspension plasma spraying: Process characteristics and applications, J. Therm. Spray Technol. 19 (1–2) (2010) 219–225.

[8] M. Marr, O. Kesler, Permeability and microstructure of suspension plasma-sprayed YSZ electrolytes for SOFCs on various substrates, J. Therm. Spray Technol. 21 (6) (2012) 1334–1346.

[9] A. Guignard, G. Mauer, R. Vassen, D. Stöver, Deposition and characteristics of submicrometer–structured thermal barrier coatings by suspension plasma spraying, J. Therm. Spray Technol. 21 (3–4) (2012) 416–424.

[10] G. Mauer, A. Guignard, R. Vassen, Plasma spraying of efficient photoactive TiO_2 coatings, Surf. Coat. Technol. 220 (2013) 40–43.

[11] R. Tomaszek, L. Pawlowski, L. Gengembre, J. Laureyns, A. Le Maguer, Microstructure of suspension plasma sprayed multilayer coatings of hydroxyapatite and titanium oxide, Surf. Coat. Technol. 201 (16–17) (2007) 7432–7440.

[12] R.B. Heimann, Plasma–spray coating, second ed., Wiley–VCH, 2008.

[13] A. Rico, P. Poza, J. Rodríguez, High temperature tribological behavior of nanostructured and conventional plasma sprayed alumina-titania coatings, Vac. 88 (1) (2013) 149–154.

[14] R. Yilmaz, A.O. Kurt, A. Demir, Z. Tatli, Effects of TiO_2 on the mechanical properties of the Al_2O_3–TiO_2 plasma sprayed coating, J. Eur. Ceram. Soc. 27 (2–3) (2007) 1319–1323.

[15] R. Tomaszek, L. Pawlowski, J. Zdanowski, J. Grimblot, J. Laureyns, Microstructural transformations of TiO_2, Al_2O_3+13TiO_2 and Al_2O_3+40TiO_2 at plasma spraying and laser engraving, Surf. Coat. Technol. 185 (2–3) (2004) 137–149.

[16] S. Guessasma, M. Bounazef, P. Nardin, T. Sahraoui, Wear behavior of alumina-titania coatings: Analysis of process and parameters, Ceram. Int. 32 (1) (2006) 13–19.

[17] E.H. Jordan, M. Gell, Y.H. Sohn, D. Goberman, L. Shaw, S. Jiang, M. Wang, T.D. Xiao, Y. Wang, P. Strutt, Fabrication and evaluation of plasma sprayed nanostructured alumina–titania coatings with superior properties, Mater. Sci. Eng. A 301 (1) (2001) 80–89.

[18] J. Ahn, B. Hwang, E.P. Song, S. Lee, N.J. Kim, Correlation of microstructure and wear resistance of Al_2O_3–TiO_2 coating plasma sprayed with nanopowders, Metall. Mater. Trans. A 37 (2006) 1851–1861.

[19] X. Lin, Y. Zeng, S.W. Lee, C. Ding, Characterization of alumina–3 wt% titania coating prepared by plasma spraying of nanostructured powders, J. Eur. Ceram. Soc. 24 (2004) 627–634.

[20] G. Darut, E. Klyatskina, S. Valette, P. Carles, A. Denoirjean, G. Montavon, H. Ageorges, F. Segovia, M.D. Salvador, Architecture and phases composition of suspension plasma sprayed alumina–titania sub–micrometer–sized coatings, Mater. Lett. 67 (1) (2012) 241–244.

[21] P. Carpio, E. Rayón, L. Pawlowski, A. Cattini, R. Benavente, E. Bannier, M.D. Salvador, E. Sánchez, Microstructure and indentation mechanical properties of YSZ nanostructured coatings obtained by suspension plasma spraying, Surf. Coat. Technol. 220 (2013) 237–243.

[22] D. Waldbillig, O. Kesler, The effect of solids and dispersant loadings on the suspension viscosities and deposition rates of suspension plasma sprayed YSZ coatings, Surf. Coat. Technol. 203 (15) (2009) 2098–2101.

[23] E. Rayón, V. Bonache, M.D. Salvador, E. Bannier, E. Sánchez, A. Denoirjean, H. Ageorges, Nanoindentation study of the mechanical and damage behaviour of suspension plasma sprayed TiO_2 coatings, Surf. Coat. Technol. 206 (10) (2012) 2655–2660.

[24] M. Vicent, E. Sánchez, T. Molina, M.I. Nieto, R. Moreno, Comparison of freeze drying and spray drying to obtain porous nanostructured granules from nanosized suspensions, J. Eur. Ceram. Soc. 32 (5) (2012) 1019–1028.

[25] M. Vicent, E. Sánchez, A. Moreno, R. Moreno, Preparation of high solids content nano–titania suspensions to obtain spray–dried nanostructured powders for atmospheric plasma spraying, J. Eur. Ceram. Soc. 32 (1) (2012) 185–194.

[26] M. Vicent, E. Sánchez, T. Molina, M.I. Nieto, R. Moreno, Dispersion of mixtures of submicrometer and nanometer sized titanias to obtain porous bodies, Ceram. Inter. 39 (8) (2013) 9091–9097.

[27] M. Vicent, E. Bannier, R. Benavente, M.D. Salvador, T. Molina, R. Moreno, E. Sánchez, Influence of the feedstock characteristics on the microestructure and properties of Al_2O_3–TiO_2 plasma–sprayed coatings, Surf. Coat. Technol. 220 (2013) 74–79.

[28] M. Vicent, E. Bannier, R. Moreno, M.D. Salvador, E. Sánchez, Atmospheric plasma spraying coatings from alumina-titania feedstock comprising bimodal particle size distributions, J. Eur. Ceram. Soc. 33 (15–16) (2013) 3313-3324.

[29] E. Sánchez, E. Bannier, M. Vicent, A. Moreno, M.D. Salvador, V. Bonache, E. Klyatskina A.R. Boccaccini, Characterization of Nanostructured Ceramic and Cermet Coatings Deposited by Plasma Spraying, Int. J. Appl. Ceram. Technol. 8 (5) (2011) 1136–1146.

[30] G. Bolelli, V. Cannillo, R. Gadow, A. Killinger, L. Lusvarghi, J. Rauch, M. Romagnoli, Effect of the suspension composition on the microstructural properties of high velocity suspension flame sprayed (HVSFS) Al_2O_3 coatings, Surf. Coat. Technol., 204 (8) (2010) 1163–1179.

[31] K. VanEvery, M.J.M. Krane, R.W. Trice, Parametric study of suspension plasma spray processing parameters on coating microstructures manufactured from nanoscale yttria–stabilized zirconia, Surf. Coat. Technol. 206 (8–9) (2012) 2464–2473.

[32] E.M. Levin, C.R. Robbins, H.F. McMordie, Phase diagrams for ceramist Volume I, fifth ed., The American Ceramic Society, Colombus, 1964.

[33] R.H. Perry, C.H. Chilton, Chemical engineers' handbook, fifth ed., McGraw–Hill, New York, 1973.

TABLES

Table 1. Main characteristics of the commercial suspensions and powders as provided by the suppliers

Reference	Suspensions						
	Suspension type	**Main crystalline phases**	**Solids content (wt%)**	**pH**	**Viscosity (mPa·s)**	**Mean aggregate size (nm)**	**Density at 20 °C (g/cm^3)**
AERODISP VP W630X	Nano-Al_2O_3	Transition aluminas (δ- and γ-Al_2O_3)	30.0±0.1	3.0-5.0	≤ 2000	140	1.27
AERODISP W740X	Nano-TiO_2	Anatase Rutile	40.0±0.1	5.0-7.0	≤ 1000	≤ 100	1.41

Reference	Powders					
	Powder type	**Main crystalline phases**	**Average primary particle size (nm)**	**Specific surface area (m^2/g)**	**pH in 4% dispersion**	**Purity (wt%)**
Condea	Submicron-Al_2O_3	α-Al_2O_3	350	9.5±0.5	---	99.5
P25	Nano-TiO_2	Anatase Rutile	21	50±15	3.5-4.5	99.5

Table 2. Main SPS spraying parameters

Ar (l/min)	**H_2 (l/min)**	**Arc intensity (A)**	**Spraying distance (mm)**	**Spraying velocity (m/s)**	**Suspension feed rate (ml/min)**	**Injector diameter (μm)**
37	8	700	30	1	27	150

Table 3. Hardness and modulus averaged values of coatings

Sample	**Hardness (GPa)**	**Modulus (GPa)**
N10	16±2	225±20
SN10 **SN15**	12±2	175±18

FIGURE CAPTIONS

Figure 1. Flow diagram describing the suspension preparation routes followed to obtain the three suspension feedstocks as well as references adopted

Figure 2. SEM micrographs at three magnifications of coatings obtained from N10, SN10 and SN15 (marked PMn: Partially Melted nanoparticles and PMs: Partially Melted submicron-sized particles)

Figure 3. Plot of the power required to as a function of solid content of suspension for both (water and ethanol)

Figure 4. EDX analysis of coating obtained from N10

Figure 5. XRD patterns of coatings obtained from N10, SN10 and SN15

Figure 6. Load versus penetration depth curves acquired by nanointentation of coatings

FIGURES

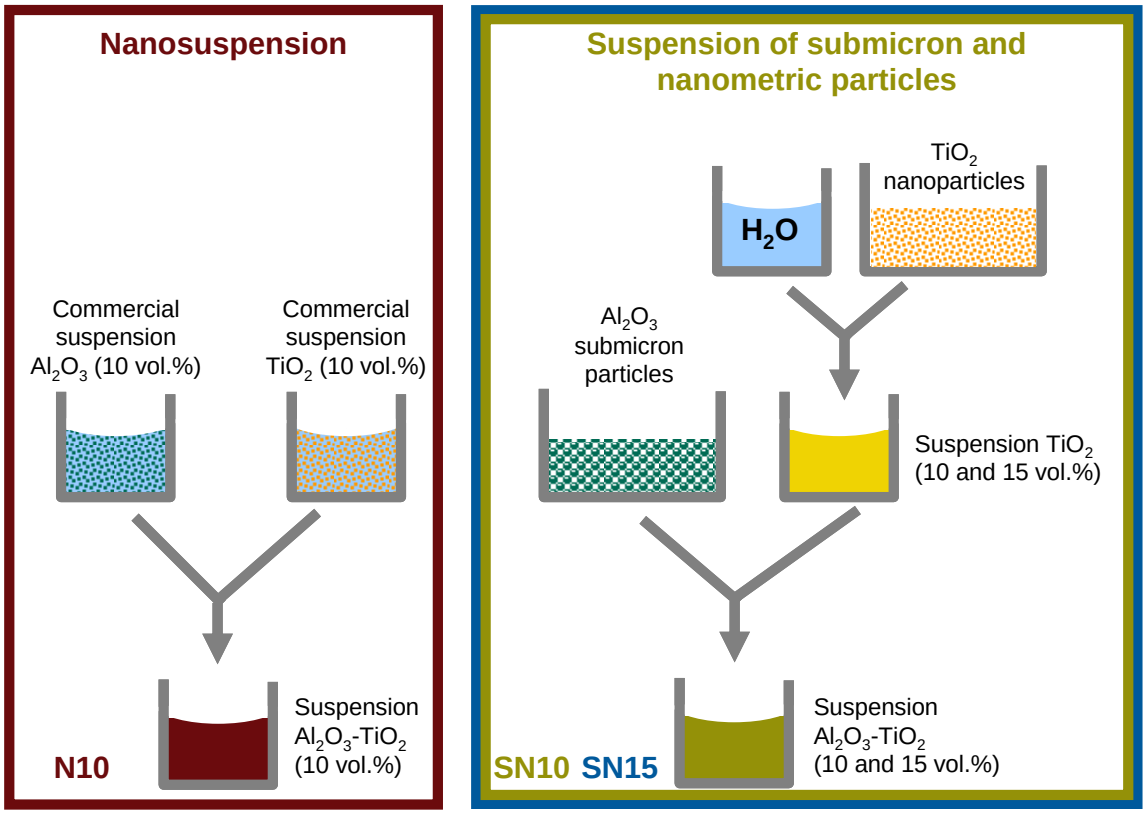

Figure 1

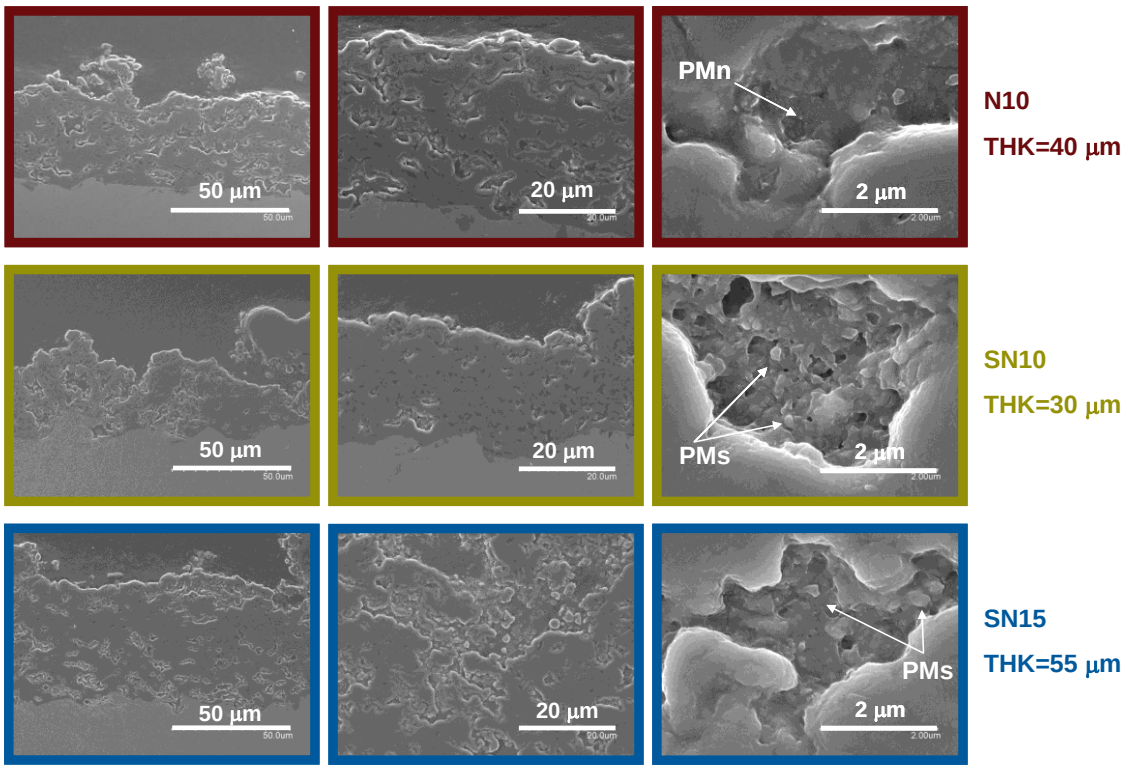
50 µm
20 µm
PMn
2 µm
N10
THK=40 µm
50 µm
20 µm
PMs
2 µm
SN10
THK=30 µm
50 µm
20 µm
PMs
2 µm
SN15
THK=55 µm

Figure 2

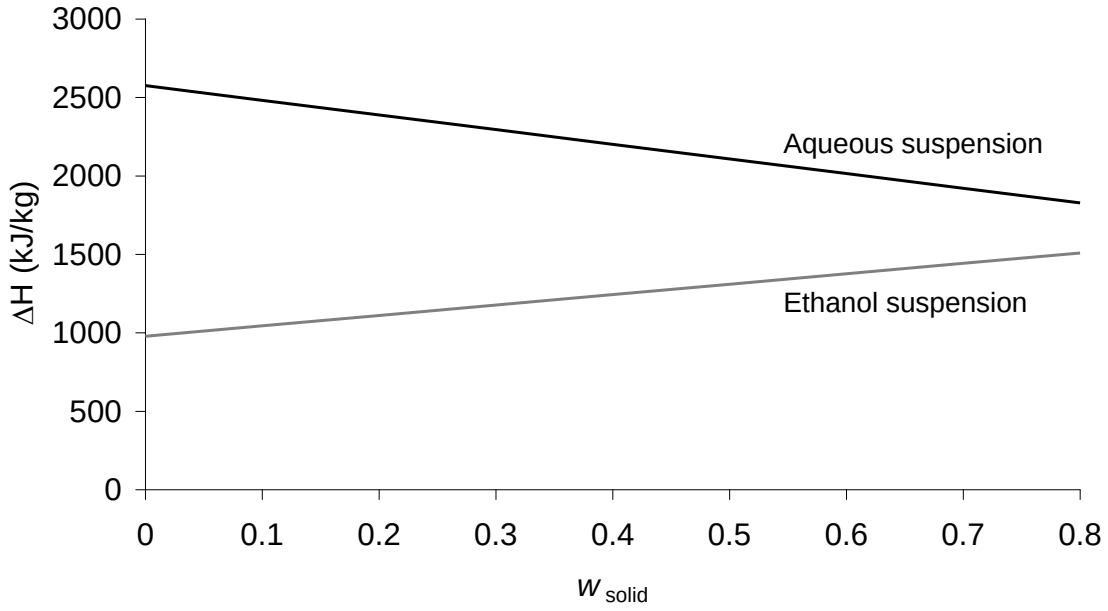
3000
2500
2000
1500
1000
500
0
ΔH (kJ/kg)
Aqueous suspension
Ethanol suspension
0
0.1
0.2
0.3
0.4
0.5
0.6
0.7
0.8
w solid

Figure 3

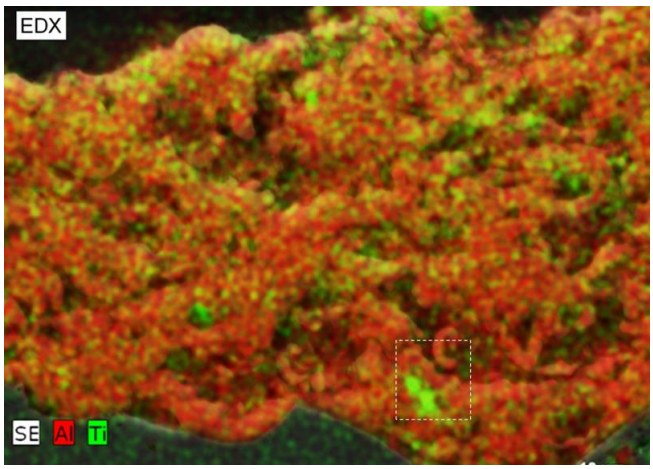

Figure 4

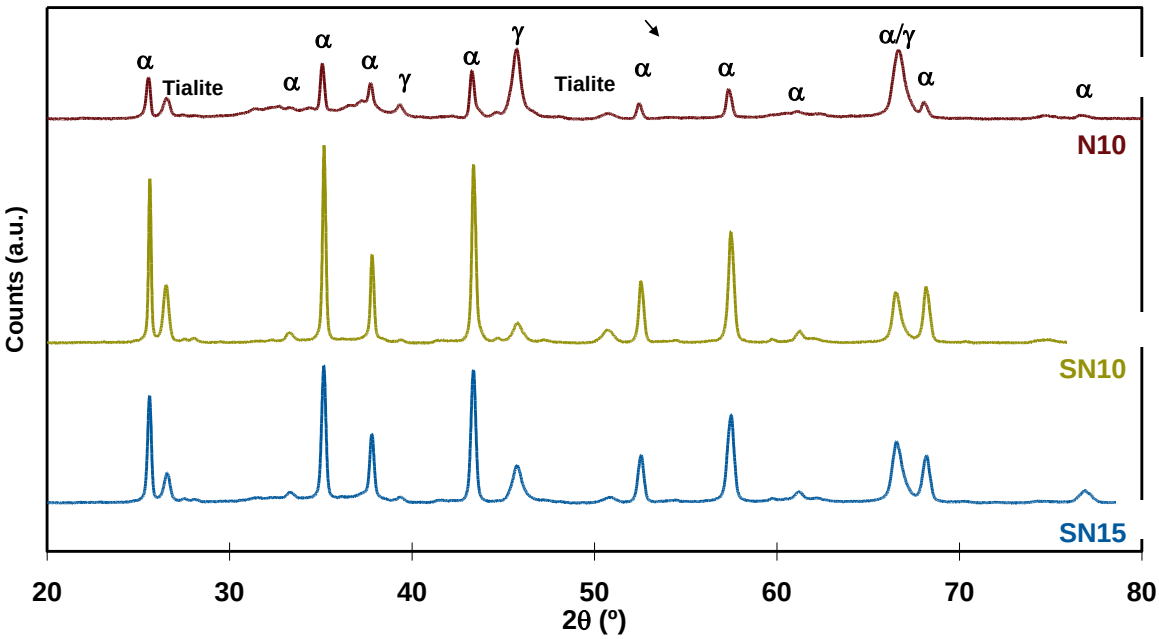
α
Tialite
α
α
α
γ
α
γ
Tialite
α
α
α
α/γ
α
α
N10
SN10
SN15
Counts (a.u.)
20
30
40
50
60
70
80
2θ (º)

Figure 5

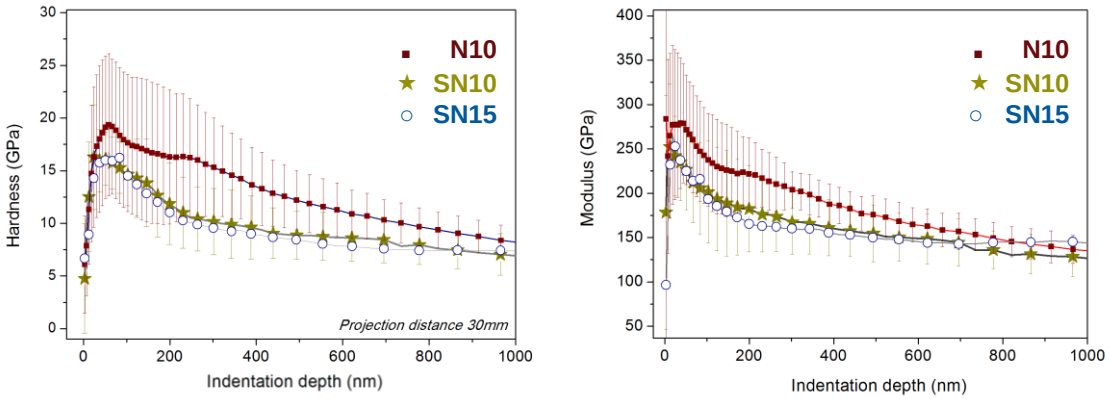
Hardness (GPa)
Indentation depth (nm)
N10
SN10
SN15
Projection distance 30mm
Modulus (GPa)
Indentation depth (nm)
N10
SN10
SN15

Figure 6